Research Article Vol. 32, No. 24 / 18 Nov 2024 / Optics Express 42347
Optics EXPRESS

UOWC spatial diversity techniques over hostile maritime environments: an approach under imperfect CSI and per-source power constraints

PEDRO SALCEDO-SERRANO,[1,*] RUBÉN BOLUDA-RUIZ,[1] JOSÉ MARÍA GARRIDO-BALSELLS,[1] ANTONIO GARCÍA-ZAMBRANA,[1] BEATRIZ CASTILLO-VÁZQUEZ,[1] ANTONIO PUERTA-NOTARIO,[1] AND STEVE HRANILOVIC[2]

[1]*Wireless Optical Communications Lab., University Institute of Telecommunication Research (TELMA), University of Málaga, CEI Andalucía Tech., Málaga E-29071, Spain*
[2]*Department of Electrical and Computer Engineering, McMaster University, Hamilton, Ontario, Canada*
[*]*pss@ic.uma.es*

Abstract: Optical communication in submarine environments has emerged as a novel technology that enables high bandwidth and high data rate links. However, the unique characteristics of the underwater channel impose new challenges, such as mitigating the remarkable absorption and scattering of hostile maritime environments. For the first time, we consider a *per-source* optical power constraint based on eye-safety regulations, which has never before been taken into account in Multiple-Input/Single-Output (MISO) systems within underwater optical wireless communication (UOWC) scenarios. Hence, we introduce an innovative spatial repetition coding (SRC) system model, which enables the analysis of an SRC scheme operating under either a *per-source* or a *per-transmitter* power constraint. In addition, a tractable generalized transmit laser selection (GTLS) model is presented in order to consider the impact of erroneous selections of the best laser source due to imperfect channel state information (CSI) at the transmitter, prevalent in underwater scenarios with dynamic fluctuations from water currents. Novel bit error rate closed-form expressions and asymptotic results are derived. The presented results demonstrate that an SRC system, when appropriately designed under a *per-source* power constraint, outperforms the TLS system by effectively mitigating the adverse effects of underwater links. Conversely, in situations where compact transmitters necessitate constraints that significantly modify eye-safety, TLS schemes are superior.

1. Introduction

The evolution of marine exploration technologies provides new insights about our oceans, such as underground flooded mines, natural gas deposits, and biological processes of marine species [1,2]. In parallel, the exponential development of the Internet of Underwater Things (IoUT) requires reliable and high-speed communication links [3,4]. Classical underwater acoustic-based communication systems suffer from bandwidth limitations and high latency, limiting the availability of real-time applications such as remote control and video streaming of underwater vehicles. In this context, underwater optical wireless communications (UOWC) represent an alternative and suitable solution due to the high data rate, and its ultra-low delay latency [5,6]. Nevertheless, recent studies have demonstrated the negative impact of the underwater channel due to the high density of small-size particles resulting in high absorption and scattering in contrast to the atmospheric medium [7–10]. In fact, the pathloss and geometric losses due to scattering limit the effective transmission often to a range of tens of meters [11]. In addition to the attenuation, oceanic turbulence-induced fading due to fluctuations in temperature and salinity has been deeply studied, revealing that its impact cannot be disregarded despite its minor

#534983 https://doi.org/10.1364/OE.534983
Journal © 2024 Received 5 Jul 2024; revised 11 Oct 2024; accepted 16 Oct 2024; published 5 Nov 2024

Optics EXPRESS

importance in realistic ocean environments [12–15]. The modeling of these impairments and their mitigation, remain crucial for the design of high-quality, practical and longer range UOWC transceivers.

Traditionally, spatial diversity techniques have been in use to mitigate fading caused by turbulence, as reported in several studies for terrestrial free-space optical communication (FSOC) [16–20] (and references therein). The scintillation effect caused by atmospheric turbulence can be effectively reduced through the use of multiple emitters at the transmitter, multiple apertures at the receiver, or a combination of both. In underwater applications, similar spatial diversity schemes have been applied directly with the aim of reducing the impact of oceanic turbulence [21–25]. In [21,22], a comprehensive UOWC channel analysis under weak oceanic turbulence modeled as a lognormal random variable performs the efficacy of a spatial repetition coding (SRC) scheme over UOWC links in terms of the bit error rate (BER). In [23], the ergodic capacity and the BER of UOWC SRC systems based on quadrature amplitude modulation is analyzed over a turbulent underwater channel described by a generalized gamma fading channel. Recently, in [24], a 2×2 UOWC MIMO system is analyzed in terms of BER under several sizes of air bubbles. In [25], an adaptive power allocation algorithm with spatial modulation is proposed to reduce the BER of a UOWC MIMO system for different types of water. In parallel with these works, a few researchers have also explored more complex spatial diversity schemes based on the selection the optical sub-path with the greatest value of channel gain [26–28]. This technique, also known as *transmit laser selection* (TLS), is critically dependent on channel state information (CSI) at the transmitter, because only the laser with the best available channel is emitting. The receiver estimates the fading channel coefficients using a CSI estimation technique, such as pilot-based, blind, or machine-learning methods [29–31]. Then, the estimated CSI is transmitted to the transmitter via a low-rate feedback link, allowing the transmitter to select the channel with the optimal performance for data transmission. The TLS scheme is in line with several studies in FSOC that aim to enhance the reliability of optical wireless systems under atmospheric turbulence channels by assuming a perfect CSI at the transmitter, which is often an unrealistic assumption in practical scenarios [32–35]. In [26], a TLS configuration with perfect CSI at the transmitter was proposed in order to extract channel full diversity and minimize the degrading effects of log normal oceanic turbulence. In [27], the outage probability of each laser of a TLS system over a vertical multi-layer cascaded Gamma-Gamma ocean turbulence channel is analyzed. In [28], the effective secrecy throughput of a UOWC system is optimized by considering a TLS scheme over a Weibull distribution oceanic turbulence considering angular pointing error. These recent studies highlight the importance of continuing research on spatial diversity schemes, such as TLS, to mitigate the different impairments of the underwater channel. However, oceanic turbulence does not represent one of the main drawbacks such as in atmospheric FSOC as compared to the beam attenuation due to absorption and scattering effects for realistic distances below 100 meters in the majority of Earth's ocean [36,37].

This paper presents the design of an SRC system specifically adapted to compensate for the effect of underwater absorption and scattering as well as the oceanic turbulence in hostile maritime environments. Additionally, we present a novel generalized TLS (GTLS) which takes into account the presence of imperfect CSI at the transmitter. Unlike [38], we propose a tractable exponential approach that models random source selections by considering a specified success probability of obtaining perfect CSI knowledge. This imperfect CSI approach allows for the modeling of a wide range of realistic scenarios where the CSI is not correctly obtained at the transmitter. The average bit error rate (ABER) is evaluated by applying the proposed SRC and GTLS strategies, considering salinity-induced oceanic turbulence channel and accounting for absorption and scattering effects with different types of water. Hence, we derive novel ABER closed-form and asymptotic expressions at high SNR as a function of the link parameters. The presented results show that an SRC system outperforms the ideal TLS as long as the SRC system is

Optics EXPRESS

designed according to the optical power constraint *per-source* conforming to eye-safety standards as introduced in this work. Furthermore, we provide compelling evidence that the performance of the TLS scheme is highly vulnerable to the presence of imperfect CSI at the transmitter. In particular, even if CSI is known at the transmitter to likelihood of greater than 90%, the TLS scheme tends to perform the SISO diversity order at high SNR. Monte Carlo simulations verify analytical and asymptotic results.

After reviewing the literature, it is evident that these works have yet to consider the mitigation of underwater attenuation in realistic scenarios through spatial diversity techniques. Therefore, an in-depth analysis of various types of water is necessary for a complete implementation, considering the unique characteristics of common underwater environments. Previous works such as [21,23] only focus on fading channels due to oceanic turbulence without comparing different turbid scenarios. In contrast, this work considers several link distances as well as different types of water such as clear ocean and coastal waters. Furthermore, MISO techniques can be exploited not only as a fading-mitigation system but also as a technique to remarkably increase the total transmitted optical power with the idea of mitigating the main degrading factors in UOWC: absorption and scattering. Hence, unlike [20–23], we present for the first time an SRC system mathematical model that enables the analysis under a *per-source* power constraint, which arise directly from eye-safety considerations and distance between laser sources. This can be accomplished by constructing the transmitter in such a novel way that only a single emitter beam is subtended by the eye at any location prescribed by the eye-safety standard, which thus far not been analyzed in the UOWC literature. Accordingly, both the SRC and TLS systems are evaluated under their maximum permissible optical power levels, as each laser diode is operated at its maximum optical power permitted by international safety standards. This novel approach permits an in-depth assessment of the impact of transmitted powers by each scheme in different water conditions and link distances. In addition, the statistical distribution for oceanic turbulence considered in the literature is limited to temperature-induced turbulence distributions usually modeled as lognormal fading channels [21,22]. This constraint reduces the field of application of the current studies because salinity gradients would be out of the analysis. For that reason, we propose to use the Weibull distribution, which has been rigorously verified using empirical data [12,39]. In addition, conventional TLS systems which rely on perfect CSI at the transmitter, though analytically interesting are impractical. In contrast to [26,27], the proposed GTLS scheme considers random errors in the feedback link, which can be result in a partial knowledge of the CSI, as well as an outdated CSI at the transmitter.

The remainder of this paper is organized as follows. In Section 2, we describe the system and channel models, including the proposed MISO structure design. In Section 3, we present and analyze the mathematical models of the SRC, and GTLS. Analytical and asymptotic closed-form expressions for the ABER are derived in Section 4. In Section 5, the proposed expressions for several realistic link configurations and water environments are evaluated. Finally, in Section 6, conclusions and future work are presented.

2. System and channel models

Consider a MISO communication structure with an array of M laser diodes (LD) equally spaced on a circular arrangement at the transmitter and a single aperture of diameter D at the receiver separated horizontally by a link span of d, as illustrated by Fig. 1. For the sake of simplicity, the receiver is assumed to be positioned at the origin, with the transmitter and receiver node arranged such that all LDs are concurrently observed by the receiver, thereby ensuring optimal alignment. Intensity modulation and direct detection (IM/DD) is assumed at the transmitter and receiver sides, respectively.

By employing an appropriate transmitter design, the typical average power constraint *per-transmitter* common in RF systems [40] can be adapted to increase the total emitted optical power

Optics EXPRESS

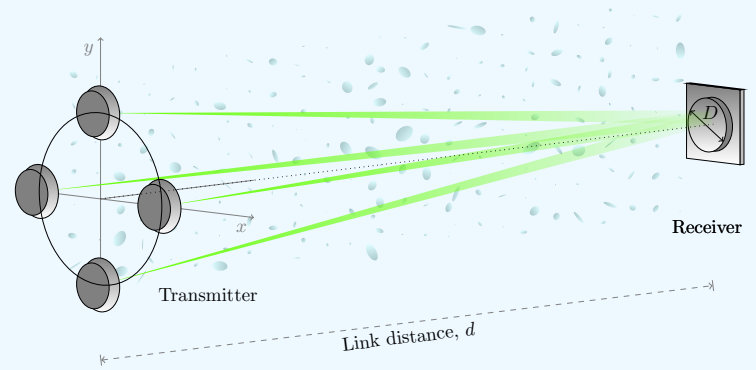

Fig. 1. Diagram of the proposed underwater MISO system.

and mitigate the severe impact of the scattering on UOWC systems in order to achieve higher performance. According to the International Electrotechnical Commission (IEC) standards, the average transmit optical power P_t is obtained from the maximum permissible exposure definition in a $\phi_p = 7$ mm diameter pupil at a distance of 100 mm [41,42]. As shown in Fig. 2, a distance between emitters, d_t, ensures that an eye near the transmitter subtends only a single emitter. Thanks to this new approach for UOWC MISO transmitters, the eye-safety constraint is satisfied in any location, so the average power P_t can be imposed *per-source*. To ensure this condition holds, assume $d_t \geq \phi_p + w_z$, where w_z is the beamwidth at 100 mm. The beamwidth can be calculated as $w_z \approx \theta \cdot 0.1$, where θ is the LD divergence angle in radians. Here, assume a symmetric LD divergence angle for the horizontal and vertical planes of 12 mrad, so that $d_t \geq$ 8.2 mm to ensure the eye-safety *per-source*. This condition represents a coherent and realistic physical limitation in commercial UOWC systems with similar circular arrangements of emitters, such as the Sonardyne BlueComm 200 [2]. The minimum distance requirement between LD emitters ensures compliance with eye safety regulations in MISO systems, regardless of the maximum output power of a specific laser, which is governed independently by the IEC standard. It should be noted that this procedure has been employed in commercial terrestrial FSOC systems but has not yet been analyzed in the existing literature of UOWC MISO systems [43].

The corresponding underwater channel is mathematically described by a composed channel gain which accurately models the impact of the oceanic losses due to the light propagation, L, and the fading induced by oceanic turbulence, h_o. On one hand, the oceanic path loss includes the effect of the absorption and scattering, as well as the geometric losses for an LD. As demonstrated [11], a complete formula to compute it is given by

$$L = A_0 \times e^{-\alpha \cdot c \cdot d}, \tag{1}$$

where $A_0 = \left(\text{erf}\left[\frac{\sqrt{\pi}}{\sqrt{2}\overline{w_z}}\right]\right)^2$ is the fraction of Gaussian beam geometric losses, $\overline{w_z} = w_z/a_r$ is the normalized beamwidth, a_r is the receiver radius, $\text{erf}[\cdot]$ is the error function, α is a correcting factor in order to consider true received power due to scattering, and c is the extinction coefficient of the water [11,44]. Table 1 summarizes two common marine environments in terms of c as the sum of the absorption, a, and scattering, b, coefficients when $\lambda = 532$ nm is assumed [5]. On the other hand, as proposed in [12,39], here we model the oceanic turbulence, h_o, using the Weibull probability distribution due to its high accuracy for different levels of salinity-induced oceanic turbulence in experimental measurement data, as follows

$$f_{h_o}(h_o) = \frac{\beta_1}{\beta_2}\left(\frac{h_o}{\beta_2}\right)^{\beta_1 - 1} \times e^{-\left(\frac{h_o}{\beta_2}\right)^{\beta_1}}, \quad h_o \geq 0, \tag{2}$$

Optics EXPRESS

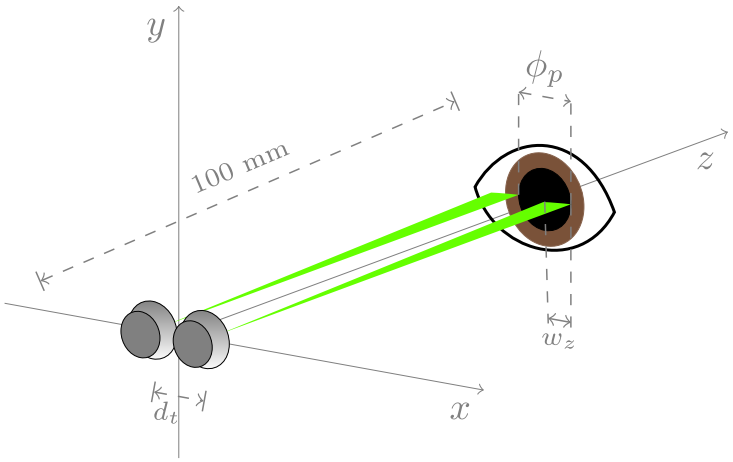

Fig. 2. Geometric representation of the minimum distance between emitters to guarantee the eye-safety regulations when some emitters are simultaneously operating under a *per-source* power constraint.

where $\beta_1 > 0$ is a shape parameter related to the strength of the oceanic turbulence-induced fading, and $\beta_2 > 0$ is a scale parameter which is related to the mean value of the received power [9]. The strength of the oceanic turbulence-induced fading is described by the scintillation index $\sigma^2_{h_o}$ by making use of the Nikishov oceanic turbulence power spectrum. A comprehensive understanding about the analytical power spectrum model and its parameters can be found in [45]. The considered numerical values of parameters are summarized in Table 2. In order to deal with several strengths of oceanic turbulence, the unitless salinity-balance parameter w is evaluated within the interval $[-5, 0]$ [46].

Table 1. Attenuation coefficients.

Type of water	$a + b = c\ [m^{-1}]$
Clear ocean water	0.114 + 0.037 = 0.151
Coastal water	0.179 + 0.219 = 0.398

Table 2. Numerical values of oceanic turbulence parameters.

Parameter	Value
Dissipation of turbulent kinetic energy (ϵ)	10^{-6} m^2/s^3
Dissipation of temperature (χ_T)	10^{-4} K^2/s
Kolmogorov length scale (η)	10^{-3} m
A_T	1.863×10^{-2}
A_S	1.9×10^{-4}
A_{TS}	9.41×10^{-3}

3. UOWC MISO channel models

In this section, mathematical models of SRC and TLS systems are derived in terms of the channel attenuation and the salinity-induced oceanic turbulence. It must be highlighted that d_t is larger than the spatial coherence radius, which is on the order of millimeters in the considered

Optics EXPRESS

scenarios. As a result, predominant salinity fluctuations are supposed and uncorrelated fading can be assumed at the receiver [47]. Furthermore, the underwater losses L can be considered identical for all emitters due to the ratio between d_t and the link distance.

3.1. Spatial repetition coding, SRC

Considering a suitable transmitter structure under the design assumption presented in Fig. 2, the photocurrent at the receiver for the proposed SRC system can be expressed as follows

$$y = x\frac{\rho}{M}LR\underbrace{\sum_{i=1}^{M} h_{o_i}}_{h_{\mathrm{SRC}}} + z, \tag{3}$$

where $1 \leq \rho \leq M$, x is the LD optical intensity, R is the photodetector responsivity which is assumed to be the unity, and h_{o_i} is the optical intensity fluctuation through the optical path between the i-th transmit LD source and the receiver. The noise at the receiver, denoted as z, primarily originates from the photodetector and includes shot and thermal noise. Although solar background noise may slightly affect UOWC links in clear ocean waters at very shallow depths, shot and thermal noise are typically the most significant noise sources due to the high absorption effect of solar background noise, especially in turbid waters [48]. As noted in [49,50], when the optical intensity is high, i.e., meaning the number of photons at the receiver becomes large, shot noise can be accurately modeled by an infinity sum of many independent Poisson distributed random variables, which approaches to a Gaussian distribution by the central limit theorem. Additionally, thermal noise, which is independent of the received optical signal, is also modeled as a Gaussian distribution [51]. Hence, the noise is modeled as a statistically independent additive white Gaussian random process which is characterized by a variance $N_0/2$ and a zero mean.

Unlike current UOWC MISO literature, the proposed system allows for adjustment between a *per-source* power constraint and a *per-transmitter* power constraint. Specifically, in the scenario where $\rho = 1$, the optical intensity at each source is restricted such that it is divided by the total number of LD sources, denoted by M, resulting in an transmitted optical intensity of $x \cdot \frac{1}{M}$. This configuration assumes an average power constraint *per-transmitter*. Conversely, when $\rho = M$, each LD operates at its maximum optical intensity, resulting in an transmitted optical intensity of $x \cdot \frac{M}{M} = x$, representing a power constraint *per-source*. Hence, the proposed SRC scheme can reduce the negative effect of scattering as the leading adverse factor in hostile maritime environments by using the maximum power of each source when a power constraint *per-source* is considered. Consequently, the resulting total transmitted optical power is $M \cdot P_t$, by increasing the maximum optical power with respect to the common approaches in theoretical analysis of SRC systems based on a power constraint *per-transmitter* considered in the literature. However, the transmitter can optimize ρ to preserve the emitted power, considering the inherent energy limitations of autonomous underwater vehicles (AUV) that are typically powered by batteries.

Regarding the form of the composite fading coefficient, while an accurate PDF of h_{SRC} was obtained in [52] as an infinite summation, this form is not tractable for the analysis of the performance of SRC schemes in terms of the channel parameters, such as the severity of the oceanic turbulence and the link distance. In order to address this inconvenience, the PDF in (2) can be approximated by a tractable single polynomial term using the Taylor expansion, such as $f_{h_o}(h_o) \doteq \frac{\beta_1}{\beta_2}\left(\frac{h_o}{\beta_2}\right)^{\beta_1-1}$. In Section 5, it will be demonstrated that the proposed approximation achieves satisfactory results without compromising the accuracy of the outcomes. By assuming independent and identically distributed fading channels, the PDF $f_{h_{\mathrm{SRC}}}(h)$ can be obtained by

Optics EXPRESS

using the moment generating function and the Inverse Laplace Transform as follows [53]

$$f_{h_{\mathrm{SRC}}}(h) \doteq \left(\frac{\beta_1}{\beta_2^{\beta_1}}\Gamma(\beta_1)\right)^{M} \frac{h^{M\beta_1-1}}{\Gamma(M\beta_1)}, \tag{4}$$

where $\Gamma(\cdot)$ is the Gamma function.

3.2. Generalized transmit laser selection, GTLS

In this subsection, we present a generalized TLS (GTLS) system, which contains both the ideal TLS scheme analyzed in the literature as well as the incorporation of imperfect CSI at the transmitter. In contrast to the SRC scheme shown in Fig. 3, a TLS scheme transmits utilizing a single source at a given time instant, while the remaining sources remain idle, as shown in Fig. 4.

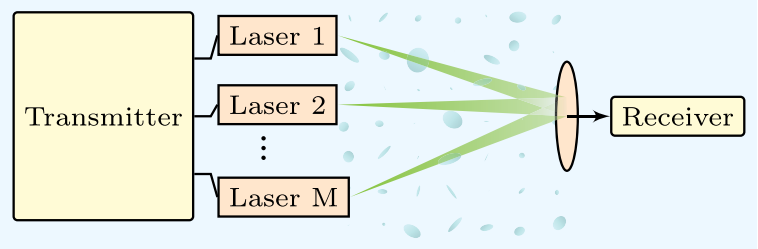

Fig. 3. Block diagram of the proposed SRC system.

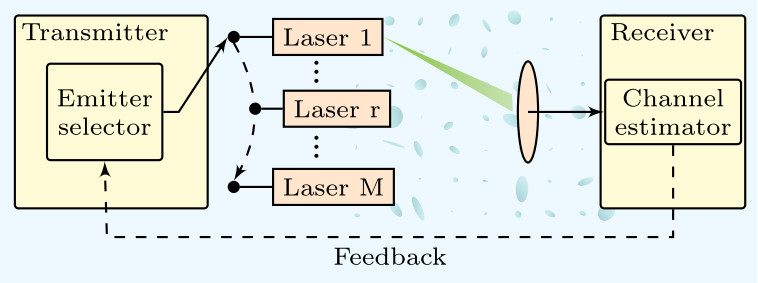

Fig. 4. Block diagram of the proposed TLS system.

In atmospheric TLS schemes, the CSI is usually sent to the transmitter node by a RF low-rate feedback channel [32,34]. However, the use of RF feedback links is not a viable option in underwater environments due to the significant attenuation of RF signals in seawater. Here, an acoustic feedback link is proposed as its low data rate and propagation delay are not problematic for underwater TLS systems, given the slow-fading nature of underwater optical power fluctuations and the relatively short to moderate link distances [54,55].

According to the existing UOWC literature, to the authors' knowledge, there has been no work on realistic implementation of a TLS system in an underwater setting. In this regard, consider imperfect CSI knowledge at the transmitter due to errors in the feedback link and/or outdated CSI. In practice, due to imperfect CSI knowledge, the transmitter eventually transmits with an LD from a set of available options. According to the order statistics, the transmitter selects the r-th smallest channel gain, where $1 \leq r \leq M$ and $r \in \mathbb{N}$. In this sense, the largest order statistic is represented by the M-th smallest channel gain. Hence, the ideal TLS scheme is modeled when

Optics EXPRESS

$r = M$, i.e., the channel with the largest gain is always selected. The PDF of h_o given the r-th smallest channel gain can be described as follows [56, Eq. (2.1.3)]

$$f_{h_{o_r}}(h \mid r) = \frac{M!}{(r-1)!(M-r)!} \frac{\beta_1}{\beta_2^{\beta_1}} h^{\beta_1 - 1} \times \sum_{k=0}^{r-1} (-1)^k \binom{r-1}{k} \left(e^{-\left(\frac{h}{\beta_2}\right)^{\beta_1}} \right)^{(k+1+M-r)}. \tag{5}$$

In order to shed light on what channel parameters determine the TLS ABER performance, we obtain an asymptotic expression of $f_{h_{o_r}}(h \mid r)$, as previously mentioned in Section 3.1, as follows

$$f_{h_{o_r}}(h \mid r) \doteq \frac{M!}{(r-1)!(M-r)!} \frac{\beta_1}{\beta_2^{r\beta_1}} \times \sum_{k=0}^{M-r} (-1)^k \binom{M-r}{k} \frac{1}{\beta_2^{k\beta_1}} h^{\beta_1(r+k)-1}. \tag{6}$$

To model a realistic scenario, consider the possibility of random incorrect channel selections due to the degradation in the feedback channel or outdated CSI at the transmitter. Hence, r can be modeled as a non-negative discrete random variable with a finite number of probability mass points for a given mean $\mathbb{E}[r]$. Therefore, we propose to quantify the accuracy of the CSI by constraining the mean of r. According to the principle of maximum entropy, if there is no knowledge about the random variable r except the mean and non-negative constraints, the distribution of r, i.e., $f_r(r)$, should be a geometric distribution due to the fact that presents the maximum entropy under these constraints [57,58]. To the best of our knowledge, this approach has not yet been considered in optical wireless communication systems. As a result, the probability of selecting the r-th smallest channel gain can be calculated as follows

$$f_r(r) = \frac{e^{l \cdot r}}{\sum_{i=1}^{M} e^{l \cdot i}}, \tag{7}$$

where l is the growth constant. It should be noted that the normalization of the exponential ensures $\sum_{r=1}^{M} f_r(r) = 1$. Furthermore, the inherent flexibility and versatility of the exponential function allows us to model a wide range of scenarios involving imperfect CSI at the transmitter with the help of a growth constant. On the one hand, scenarios where the CSI is rarely outdated at the transmitter and obtains a high likelihood of success are associated with a larger growth constant due to the probability increases by a factor e. On the contrary, scenarios where the CSI is commonly outdated or unknown at the transmitter are described with a lower growth constant due to the fact that the whole of emitters present a similar probability of being selected. A useful perspective is to consider a success probability p_M as the probability of selecting the best channel gain, i.e., the probability of $r = M$. Consider defining the growth parameter l from a success probability p_M by performing the inversion of Eq. (7) when $r = M$. This can be numerically accomplished with the help of mathematical software packages such as Wolfram Mathematica. This correlation between the growth parameter and the success probability provides novel and valuable insights into the characteristics and implications of the CSI at the transmitter in the system performance. In Fig. 5, the proposed approach is computed for different success probabilities of obtaining a perfect CSI at the transmitter. As can be observed, our novel approach encompasses a spectrum of scenarios, covering the entire range between the two extreme cases. In the worst case of imperfect CSI, which is equivalent to an absence of CSI, the transmitter uniformly selects an emitter, i.e., $p_M = \frac{1}{M}$, which is described by $l = 0$. Otherwise, the case

Optics EXPRESS

of having always perfect CSI at the transmitter (best case), i.e., $p_M = 100\%$, is described by $l \to \infty$. In practice, an l greater than 4.6 is enough to obtain a $p_M \geq 99\%$, as shown in Fig. 5. As mentioned above, $\mathbb{E}[r]$, p_M and l provide the same information regarding the CSI at the transmitter. However, for the reader's convenience, throughout the remainder of the article, only the probability of selecting the best channel gain p_M will be used. Hence, the PDF of the proposed GTLS can be obtained by averaging (7) in (5) as follows

$$f_{h_{\text{GTLS}}}(h) = \sum_{r=1}^{M} f_r(r) \cdot f_{h_{o_r}}(h \mid r). \tag{8}$$

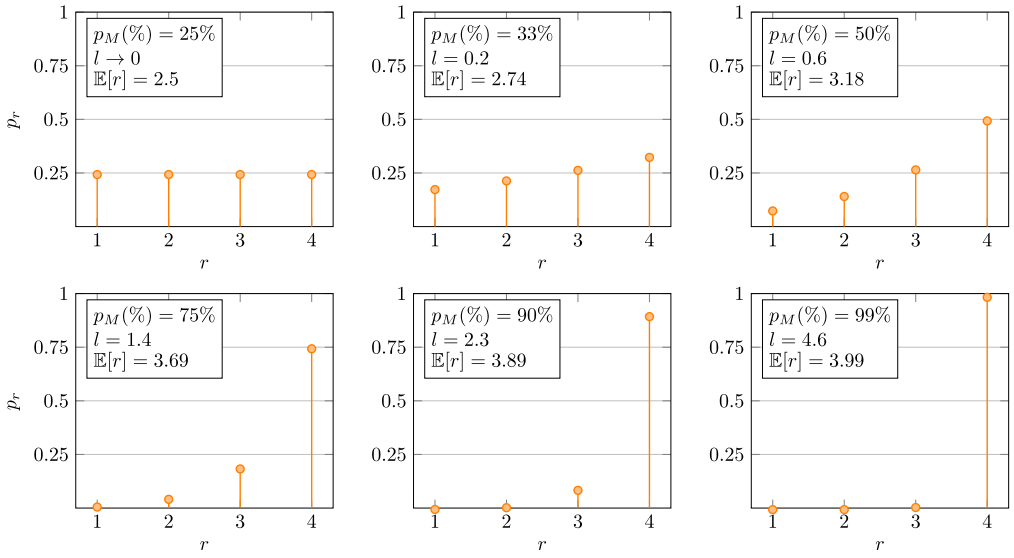

Fig. 5. Probability mass function of r with 4 laser sources.

4. BER performance of MISO systems

In this section, the ABER performance of UOWC systems is analyzed when using the proposed MISO schemes and on off keying (OOK) modulation under the composite fading channel. It should be noted that non-return-to-zero (NRZ) OOK modulation is assumed due to its lower bandwidth requirements. Furthermore, it is assumed that the CSI is perfectly known at the receiver. As stated in [59], the conditional ABER at the receiver for the case of equally likely transmitted symbols and a SISO system can be calculated as follows

$$P_b(E|h) = Q\left(\sqrt{2}\gamma \cdot L \cdot h_o\right), \tag{9}$$

where $Q(\cdot)$ represents the Gaussian-Q function, $\gamma = P_t\sqrt{T_b}/\sqrt{2}\sigma_n$ is the normalized optical SNR in the absence of fading, and T_b is the bit period. The ABER is determined by taking the average of the PDF $f_{h_o}(h)$ as follows

$$P_b = \int_0^{\infty} Q\left(\sqrt{2}\gamma \cdot L \cdot h\right) \cdot f_{h_o}(h)\, dh. \tag{10}$$

Optics EXPRESS

4.1. SRC performance

The corresponding ABER of the MISO UOWC channel with SRC scheme can be calculated as

$$P_{b_{\mathrm{SRC}}} = \underbrace{\int_0^\infty \cdots \int_0^\infty}_{M} Q\left(\sqrt{2}\gamma \cdot \frac{\rho L}{M} \sum_{i=1}^{M} h_i\right) \prod_{i=1}^{M} f_{h_{o_i}}(h_i)\, dh_i. \tag{11}$$

Unfortunately, as far as we know, (11) is mathematically intractable. Hence, the asymptotic ABER solution at high SNR can be derived by using (4) to gain novel insights into the dominant factors that impact on the ABER performance when using the SRC system. The ABER behaves asymptotically as $P_b \doteq (G_c\gamma)^{-G_d}$, where G_c and G_d denote the coding gain and diversity order, respectively [60]. Hence, by substituting (4) into (11), a closed-form asymptotic expression can be easily derived as follows

$$P_{b_{\mathrm{SRC}}} \doteq \frac{\left(\beta_1 \left(\frac{\beta_2 L\rho}{M}\right)^{-\beta_1} \Gamma(\beta_1)\right)^M}{2^{1+M\beta_1}\Gamma\left(\frac{M\beta_1}{2}+1\right)} \gamma^{\frac{-\beta_1}{2}M}. \tag{12}$$

4.2. GTLS performance

The corresponding ABER of the MISO UOWC channel with a GTLS scheme can be estimated as

$$P_{b_{\mathrm{TLS}}} = \int_0^\infty Q\left(\sqrt{2}\gamma \cdot L \cdot h\right) f_{h_{o_r}}(h \mid r)\, dh. \tag{13}$$

By substituting (5) into (13) and using [61, Eq. (07.34.21.0012.01)] and [61, Eq. (06.27.26.0006.01)], the ABER performance of a GTLS system, which transmits through the r-th smallest channel gain, is obtained as follows

$$\begin{aligned} P_{b_{\mathrm{TLS}}}(r) = {} & \frac{\beta_1 M!}{(r-1)!(M-r)!} \frac{\sum_{k=0}^{r-1}(-1)^k \binom{r-1}{k}}{4\sqrt{\pi}\left(\beta_2 L\sqrt{\gamma}\right)^{\beta_1}} \\ & \times H_{2,2}^{1,2}\left(\frac{k+M-r+1}{\left(\sqrt{\gamma}L\beta_2\right)^{\beta_1}} \middle| \begin{matrix} \left(\frac{1-\beta_1}{2}, \frac{\beta_1}{2}\right), \left(1-\frac{\beta_1}{2}, \frac{\beta_1}{2}\right) \\ (0,1), \left(\frac{-\beta_1}{2}, \frac{\beta_1}{2}\right), \end{matrix}\right), \end{aligned} \tag{14}$$

where $H_{m,n}^{p,q}(\cdot)$ is the H-Fox function [62, Eq. (1.1.1)]. Similarly to the SRC scheme, the corresponding asymptotic solution is calculated by replacing (6) into (13) as

$$P_{b_{\mathrm{TLS}}}(r) \doteq \frac{M!}{r!(M-r)!} \frac{\Gamma\left(\frac{1}{2}(r\beta_1+1)\right)}{2\sqrt{\pi}(\beta_2 L)^{r\beta_1}} \gamma^{\frac{-\beta_1}{2}r}. \tag{15}$$

Based on the approach proposed in (7), the ABER performance of a GTLS system can be expressed as a function of the growth parameter l by averaging in r as follows

$$P_{b_{\mathrm{GTLS}}} = \sum_{r=1}^{M} f_r(r) \cdot P_{b_{\mathrm{TLS}}}(r). \tag{16}$$

In the same way, the asymptotic ABER performance of a GTLS system can be calculated by substituting the asymptotic expression of $P_{b_{\mathrm{TLS}}}$ proposed in (15) into (16).

Optics EXPRESS

5. Numerical results

In this section, we assess the performance of the ABER for SRC and GTLS techniques in various realistic UOWC scenarios. Firstly, we compute the ABER expressions for clear ocean and coastal water environments to determine the benefits of these spatial diversity techniques under different scattering conditions. It is worth mentioning that harbor water scenarios have been excluded due to their high losses, which limit the maximum achievable distance to less than 15 meters [11]. Therefore, we consider practical link spans such as $d = \{30, 50, 60\}$ m and $d = \{20, 30, 35\}$ m for clear ocean and coastal waters, respectively. Moreover, the parameters β_1 and β_2 are calculated when the salinity-balance parameter $w = -1$, which represents an hostile salinity-induced oceanic turbulence scenario [10,46]. In order to establish the baseline ABER performance, we also include the ABER performance of a SISO UOWC system. Furthermore, the ABER results of the conventional SRC and ideal TLS schemes are calculated to analyze the differences between the two proposed MISO schemes and the previously reported results of SRC and TLS schemes in the literature.

Monte Carlo simulations verify analytical and asymptotic results. The proposed simulation platform consider 10^{10} bits to ensure a BER precision up to of 10^{-9} [63]. The range of SNR considered is directly related to providing a practical average BER analysis below 10^{-6} and up to 10^{-9}, which is considered a standard range benchmark in optical communication systems for robust data transmission and a practical error-free information rate. At the receiver side, the transmitted signal is detected using a matched filter, which maximizes the sampled SNR, and a maximum likelihood detector is employed to minimize symbol error probability. The remainder of configuration parameters are summarized in Table 3.

Table 3. UOWC system parameters.

Parameter	Symbol	**Value**
LD divergence angle	θ	12 mrad
Wavelength	λ	532 nm
Photodetector surface diameter	D	20 cm
Photodetector field-of-view	-	180°
Salinity-balance parameter	w	-1 (unless specified otherwise)
Number of LDs	M	4 (unless specified otherwise)
Distance between emitters	d_t	8.2 mm
SRC balance parameter	ρ	[0, 1]
Probability of perfect CSI at the transmitter	$p_M(\%)$	[0, 100]%

In Figs. 6(a), and 6(b), we present the ABER performance of two SRC schemes and GTLS scheme with perfect CSI at the transmitter, i.e., an ideal TLS ($r = M$), when $M = 4$ laser sources are considered in clear ocean and coastal waters, respectively. The proposed SRC scheme is applied in order to increase the total emitted optical power, so we assume a *per-source* power constraint under the assumption of Fig. 2 ($\rho = M$). That is, the proposed SRC scheme transmits an optical power of P_t from each LD source, i.e., the maximum permissible average optical power. In the same way, each LD source in GTLS scheme also transmits P_t. Hence, the comparison is based on the number of sources and the transmitted optical power by each of them. In order to compare these results with conventional SRC systems that have been presented in the UOWC literature, the ABER of an SRC under a *per-transmitter* power constraint, i.e., $\rho = 1$, is also depicted.

As mentioned in Section 3, an ideal TLS is included in the proposed GTLS scheme by assuming perfect CSI ($p_M = 100\%$). As shown in Figs. 6(a), and 6(b), we demonstrate that the asymptotic

Optics EXPRESS

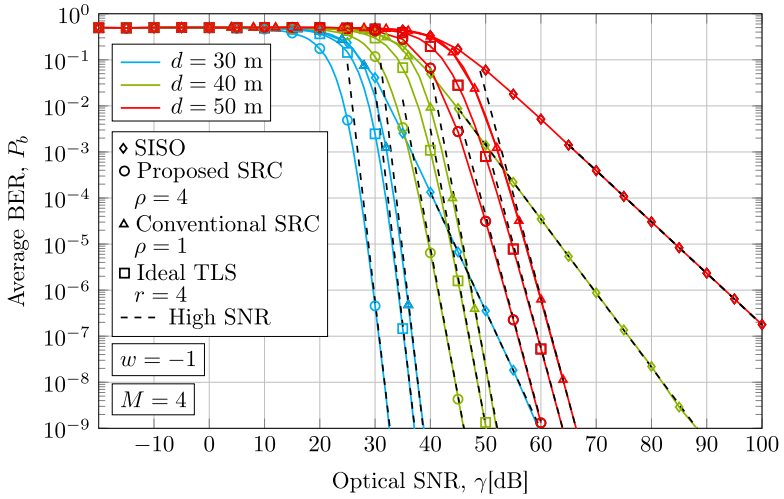

(a) Clear ocean water

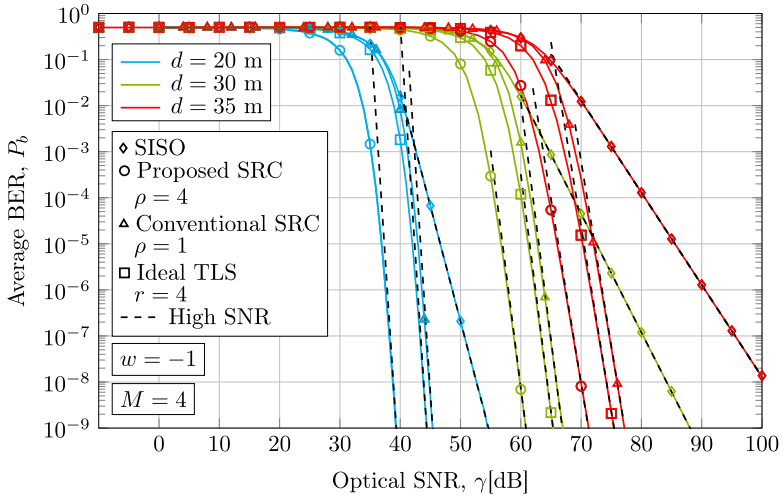

(b) Coastal water

Fig. 6. ABER in UOWC links in clear ocean (a), and coastal waters (b), under oceanic turbulence, assuming a salinity-balance of $w = -1$ and several link distances when the SRC and GTLS schemes are used with 4 emitters when perfect CSI is assumed.

expressions for ABER performance in (12) and (15) for SRC and GTLS systems, respectively, as well as the analytic ABER performance expression for GTLS scheme in (14), match closely with the Monte Carlo simulation results across the entire optical SNR regime. These results confirm the high accuracy and the usefulness of the proposed closed-form expressions in both clear ocean and coastal waters and different link distances. It is important to mention that the pathloss L is evaluated for both clear ocean and coastal waters in Figs. 6(a) and 6(b), respectively. Despite the short range of the link, the high pathloss in coastal water has a significant impact on the ABER performance. In fact, at a link distance of $d = 30$ m and a SNR of 55 dB, the ABER performance for a SISO system in clear ocean water is $P_b = 1.8 \times 10^{-8}$, while in coastal water is $P_b = 0.17$ when the same turbulence conditions are considered. Thus, it is remarked the dramatic impact of

Optics EXPRESS

scattering, which represents the main impairment for UOWC links. At the same time, Figs. 6(a), and6(b) also illustrate that the SRC technique outperforms the ideal TLS scheme in both kinds of water, despite the unrealistic assumption of having perfect CSI knowledge at the transmitter. These results highlight for the first time the advantage of using the proposed SRC system over a TLS system due to the significant impact of scattering on the UOWC channel. This is because an SRC system properly designed according to Fig. 2 is capable of transmitting more optical power with the eye-safety constraint *per-source* by using the same number of transmitters sources, as illustrated in Eq. (3) when $\rho = M$. Unlike the proposed SRC scheme, a conventional SRC system with *per-transmitter* power constraint, i.e., $\rho = 1$, obtains a higher ABER than an ideal TLS system. At a link distance of $d = 30$ m and a SNR of 60 dB, the ABER performance for the proposed SRC system in coastal water is reduced at $P_b = 7.5 \times 10^{-9}$, while in TLS scheme is $P_b = 1.19 \times 10^{-4}$ and in a conventional SRC system is $P_b = 0.012$.

As can be observed, the difference between the proposed SRC system and TLS system is reduced significantly as the link distance increases. In this regard, in order to provide further insights into the impact of the UOWC channel parameters on the ABER performance for both schemes, we can compute mathematically the gain of the proposed SRC configuration with respect to a TLS configuration, because both curves present asymptotically the same slope in a log-log scale, i.e., the same diversity order, G_d, at high SNR. In fact, in Fig. 6, it is clear that there exists a gap in the abscissa-axis between the TLS and SRC ABER curves, which shows a difference in decibels (dB) in order to achieve the same ABER performance. This gap can be asymptotically obtained using (12) and (15) to yield

$$G = \frac{10}{M\beta_1} \log_{10}\left(\left(\frac{\rho}{M}\right)^{M\beta_1} \frac{\Gamma(1+M\beta_1)}{\Gamma(1+\beta_1)^M}\right). \tag{17}$$

On the one hand, in Fig. 7, we investigate the impact of the link distance on the gain of an SRC configuration relative to a TLS scheme for different strengths of turbulence based on the salinity-balance parameter w by assuming $w = \{-3, -1\}$ when 2 and 4 laser sources are considered. On the other hand, Fig. 8 presents similar results, where the performance enhancement of the SRC versus TLS is plotted as a function of the numbers of laser sources with a salinity-balance parameters of $w = \{-3, -1\}$ and a link distance $d = \{30, 50\}$ m.

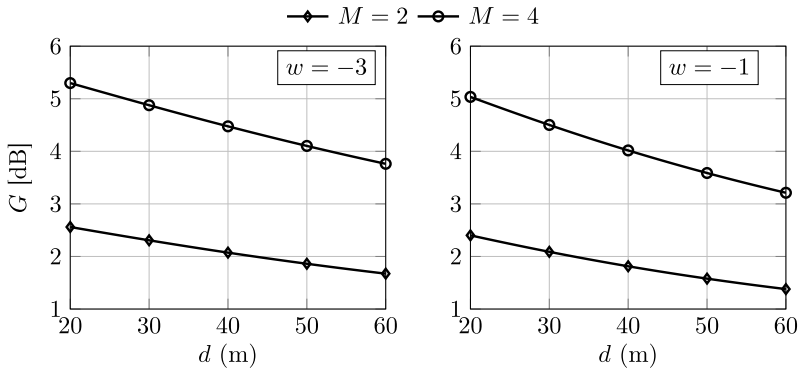

Fig. 7. The gain G in (17) of an SRC scheme compared to a TLS scheme as a function of the link span, assuming $\rho = M$ and perfect CSI when different severity of oceanic turbulence conditions and number of LD sources are considered.

Firstly, it can be observed that the performance enhancement due to diversity techniques shows different behavior for TLS and SRC schemes. It can be inferred that the coding gain of the TLS scheme increases faster than the SRC coding gain as the link distance increases. These conclusions can be extrapolated to both strength of oceanic turbulence. Therefore, the findings

Optics EXPRESS

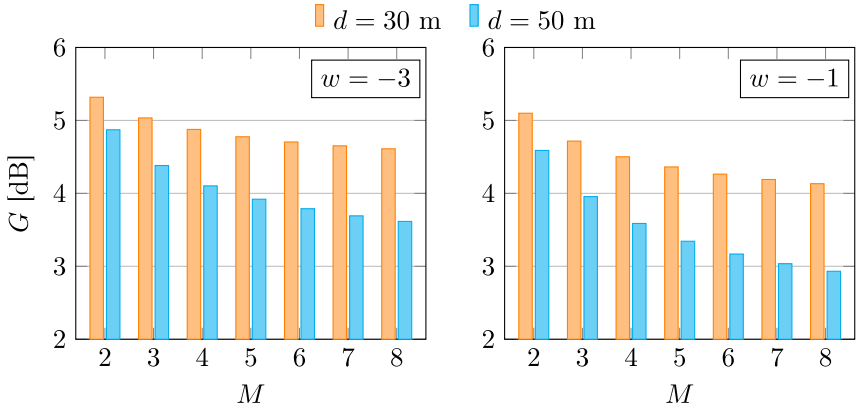

Fig. 8. The gain G as a function of the total number of transmitter sources M, assuming $\rho = M$ when different link spans are considered under different severity of oceanic turbulence.

suggest that the benefit of the SRC in comparison to the TLS scheme is likely to become less pronounced for extended link distances and a considerable number of light-emitting components. However, despite the fact that a TLS system tends to exhibit a better behavior than the SRC system at very long link distances and with several emitters, in none of the realistic analyzed scenarios does it manage to improve the coding gain of the proposed SRC system. As mentioned before, this assertion maintains validity because the SRC system is designed according to Fig. 2. If the total emitted power of the source is subjected to a *per-transmitter* constraint, the SRC system would exhibit a higher ABER than a TLS system. Unlike previous studies that neglect the importance of an appropriate transmitter structure design, our findings clearly illustrate that an alternative SRC system outperforms the TLS system in mitigating the dramatic underwater attenuation under realistic link distances and oceanic turbulence. In addition, the aforementioned findings can be employed to assess whether the performance in terms of BER of the SRC scheme provides an adequate trade-off for the higher energy consumption associated with a *per-source* power constraint, specially in battery-powered communication devices.

In Figs. 9(a), and 9(b), we show the ABER performance of a TLS scheme in which the transmitter always selects the r-th smallest channel gain due to the imperfect CSI for clear ocean and coastal water, respectively. These results provide a lower and upper bounds for the ABER performance of a TLS system which always selects the smallest channel gain and the best channel gain, respectively. It is essential to highlight that the ABER performance bounds in TLS systems has been studied in terrestrial FSOC research, but not in underwater contexts. It should also be noted that the SISO system can actually provide better performance than a TLS configuration where the emitter selector always chooses the LD with the smallest fading coefficient in both types of water. In clear ocean water at a link distance of 50 m and an optical SNR of 60 dB, the UOWC SISO system achieves an ABER performance of $P_b = 5.16 \times 10^{-3}$, while a TLS system with $r = 1$ achieves an ABER performance of $P_b = 0.02$. By comparison, a TLS system with $r = 2$ achieves $P_b = 5 \times 10^{-4}$, a TLS system with $r = 3$ achieves $P_b = 7.8 \times 10^{-6}$, and an ideal TLS achieves $P_b = 5.3 \times 10^{-8}$.

After the comprehensive ABER comparison above, we turn our attention to the performance of realistic and feasible TLS systems, in which the transmitter node randomly uses the LD with the r-th smallest channel gain due to imperfect CSI knowledge. As opposed to Figs. 9(a), and 9(b), where the transmitter consistently selects the r-th smallest channel gain due to imperfect CSI, the proposed generalization for the TLS scheme, i.e., the GTLS scheme, allows that the transmitter randomly transmits with an LD from a set of available options. Hence, in Figs. 10(a), and 10(b),

Optics EXPRESS

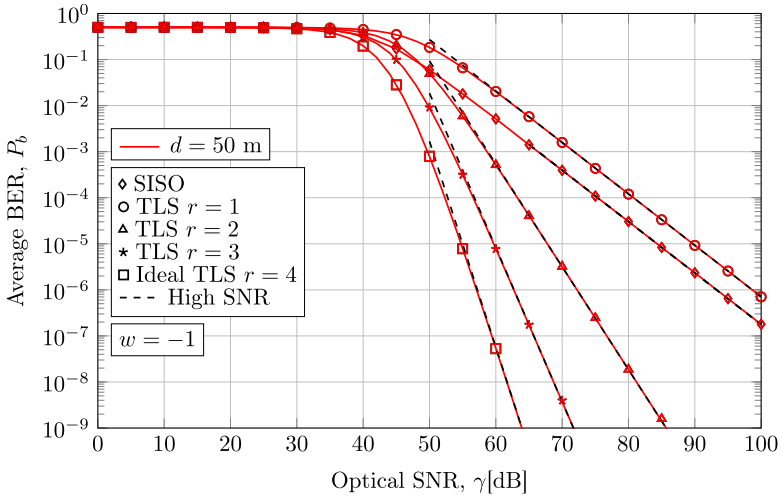

(a) Clear ocean water

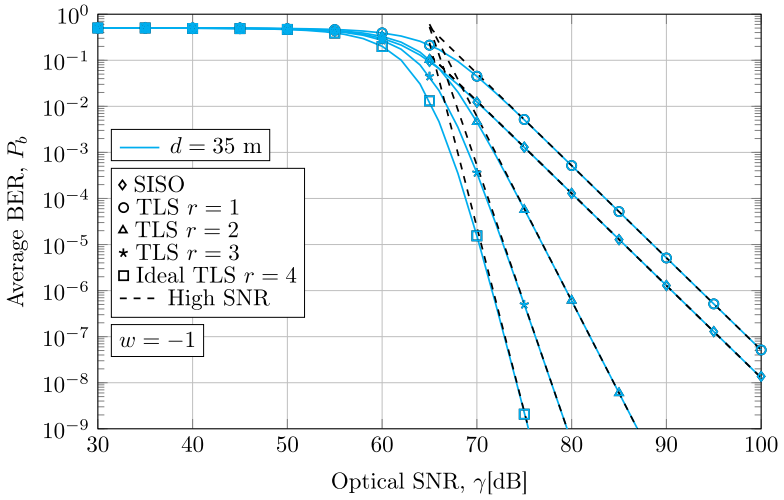

(b) Coastal water

Fig. 9. ABER in UOWC links in clear ocean (a), and coastal waters (b), under ocean turbulence, assuming a salinity-balance of $w = -1$ when an imperfect TLS scheme transmits trough the r-th smallest channel gain.

we investigate more realistically the impact of potential errors in the emitter selector block on the ABER performance of a TLS system due to an imperfect CSI at the transmitter. We consider different scenarios for several probabilities of obtaining perfect CSI at the transmitter. Here, we show scenarios with a success probability of $p_M = \{50\%, 75\%, 90\%, 99\%\}$, which is defined in (7) when considering $r = M$. According to our results, the proposed ABER performance in (16), in both its analytical and asymptotic form, closely matches the Monte Carlo simulation results, validating the usefulness of these expressions. Furthermore, as anticipated, the performance of the GTLS system is highly susceptible to imperfection in the source selection process, despite the low probability of selecting incorrect laser sources. In order to achieve the forward-error-correction (FEC) threshold of 3.8×10^{-3}, the GTLS system with $p_M = 50\%$ requires an optical SNR of

Optics EXPRESS

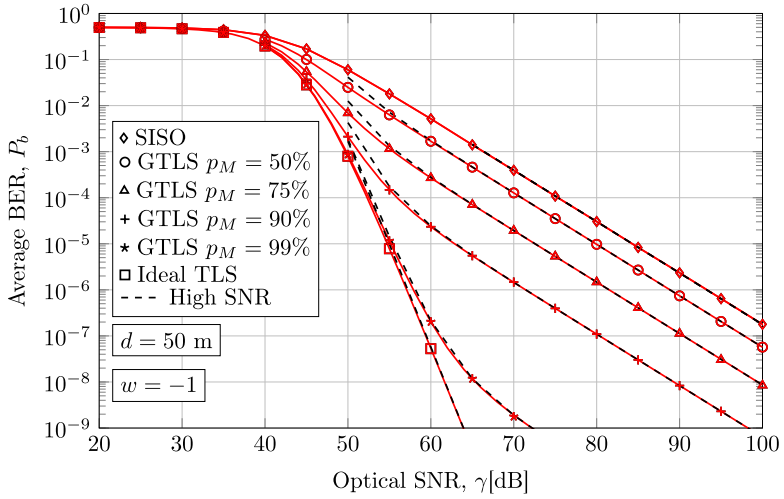

(a) Clear ocean water

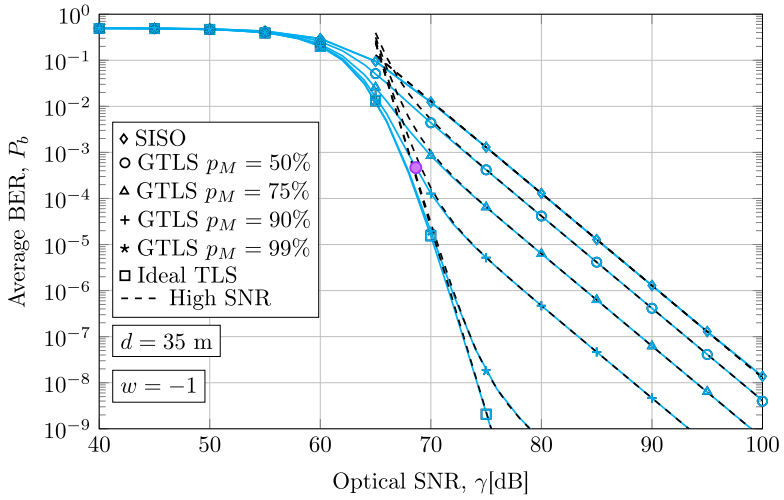

(b) Coastal water

Fig. 10. ABER in UOWC links in clear ocean (a), and coastal waters (b) when a GTLS scheme are used with 4 source lasers for several imperfect CSI at the transmitter scenarios, under salinity-induced turbulence with a salinity-balance of $w = -1$.

56 dB when a link distance of 50 m and a salinity-balance parameter of $w = -1$ are considered in clear ocean water. This represents an improvement of only 4 dB compared to the 60 dB required for a SISO system under the same environmental conditions. As expected, as the probability of obtaining perfect CSI at the transmitter increases, the gain improvement becomes more significant, with improvements of 11 dB, 21 dB, and 29 dB computed for GTLS system with $p_M = 75\%$, $p_M = 90\%$, and $p_M = 99\%$, respectively. These results contribute significantly to exactly quantify the consequence of imperfect CSI at the transmitter in TLS systems, shedding light on the practical feasibility and performance limitations of such systems. Further, the receiver is able to deduce the CSI at the transmitter from the theoretical ABER in order to enhance the feedback link. Secondly, note that the diversity order, i.e., the asymptotic slope of the ABER

Optics EXPRESS

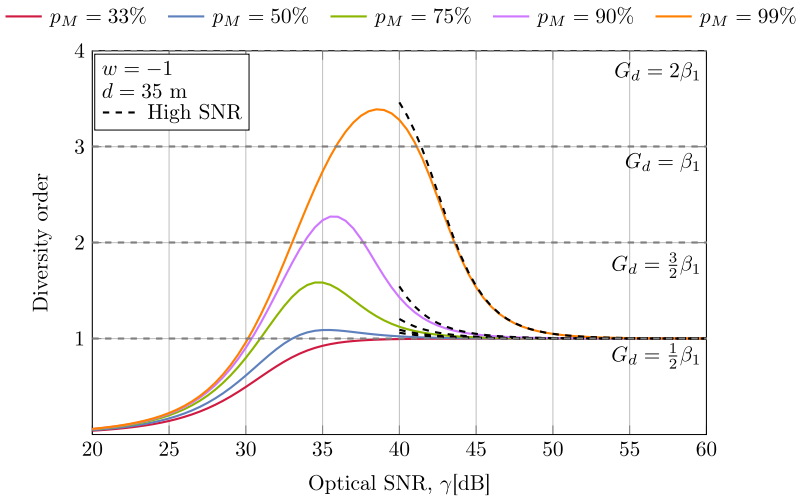

(a) Clear ocean water

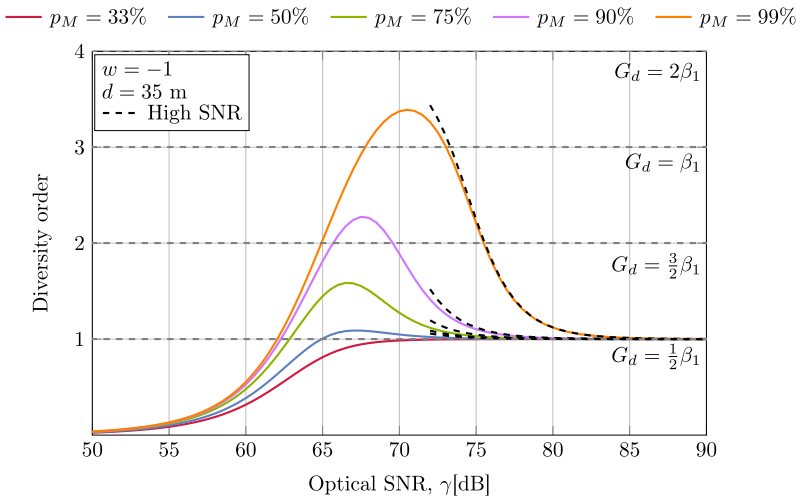

(b) Coastal water

Fig. 11. Diversity order of ABER when a GTLS scheme are used with 4 source lasers for several imperfect CSI at the transmitter scenarios in clear ocean (a), and coastal waters (b), under salinity-induced turbulence, assuming a link distance of 35 m and a salinity-balance of $w = -1$.

performance of GTLS systems, decreases as the SNR increases. Although the transmitter has a probability of obtaining the CSI exceeding 90%, the GTLS scheme exhibits a diversity order similar to that of a SISO system at high SNR.

To provide novel insights into the GTLS performance, we analyze the behavior of the diversity order as follows

$$G_d(l) = \frac{\partial P_{b_{\text{GTLS}}}(l)}{\partial \gamma}. \tag{18}$$

Optics EXPRESS

For the convenience of the reader, we do not include the non-tractable analytic expression due to its complexity. Asymptotically, we can also obtain a more tractable expression as follows

$$G_d(l) \doteq \frac{10^{\frac{\gamma}{5}}\beta_1}{2} \frac{\sum_{r=1}^{M} \frac{10^{-\frac{\gamma}{5}(1+\frac{r\beta_1}{2})} e^{l(r-1)} \Gamma\left(\frac{1}{2}(1+r\beta_1)\right)}{(M-r)!(r-1)!(L\beta_2)^{r\beta_1}}}{\sum_{r=1}^{M} \frac{10^{\frac{-\gamma r\beta_1}{10}} e^{l(r-1)} \Gamma\left(\frac{1}{2}(1+r\beta_1)\right)}{r!(M-r)!(L\beta_2)^{r\beta_1}}}. \tag{19}$$

Figures 11(a), and 11(b) provide insights about the diversity order of the ABER performance of the GTLS system with 4 laser sources for several probabilities of obtaining perfect CSI at the transmitter. We consider a salinity-balance parameter $w = -1$ and a link distance of 35 m for clear ocean and coastal waters. As a reference, the diversity order of $P_{b_{\text{TLS}}}(r)$ in (15) is also plotted for $r = \{1, 2, 3, 4\}$. It should be noted that the asymptotic expression in (19) matches accurately with analytic results at high SNR in both kinds of water. Although the probability of obtaining a perfect CSI at the transmitter is 99%, the diversity order is far from what is obtained when a perfect TLS system is considered. For the first time, it can be concluded that the full diversity gain can not be achieved with a realistic TLS system when practical oceanic turbulence scenarios are supposed, even with a $p_M = 99\%$. Furthermore, the trend of the diversity order after the peak corroborates the results obtained in Figs. 10(a), and 10(b), where the slope of the imperfect GTLS tends to the SISO slope, i.e., $G_d = \beta_1/2$. As predicted in Fig. 10, the diversity order falls earlier when p_M is low. These results confirm that an imperfect TLS is susceptible to errors in the feedback link and outdated CSI at the transmitter. As can be seen, an additional SNR is required to achieve the same G_d diversity order in coastal water as in clear ocean water with the same oceanic turbulence, which is consistent with the previous results. The inflection point of the $p_M = 90\%$ scenario is achieved at 36 dB in clear ocean water, while the same peak is obtained at 68 dB. In Fig. 10(b), the purple circle indicates the maximum diversity order achieved for the $p_M = 90\%$ case in coastal water.

6. Conclusion

This paper analyzes the ABER of MISO UOWC systems, which are designed to compensate for underwater absorption and scattering, as well as oceanic turbulence, in hostile maritime environments by employing a novel view of optical power constraint in MISO systems based on eye-safety regulations. This new perspective on optical power constraints enables a more reasonable adaptation of UOWC transceivers to underwater environments. Further, a generalized TLS system is proposed in order to consider an imperfect CSI due to feedback link errors and outdated CSI. The paper presents a novel tractable exponential approach for modeling random source selections based on the success probability of obtaining a perfect CSI at the transmitter. This is capable of modeling a wide range of scenarios by only modifying the success probability of perfect CSI. Analytical and asymptotic expressions are derived from comparing the ABER performance with SRC and GTLS strategies over realistic oceanic scenarios. According to the results obtained here, the SRC system, with an appropriate structural design, outperforms the TLS system due to the its ability to effectively reduce the negative impact of absorption and scattering. Hence, in scenarios with flexibility in the transmitter design which allows for enough distance between sources and allows a *per-source* optical power constraint, the use of SRC emerges as the preferable option. Conversely, in situations characterized by compact transmitters mandating distance between sources constraints, it is recommended to use TLS schemes. In addition, in accordance with the GTLS analysis, the ABER performance of a GTLS system is very susceptible to imperfect CSI at the transmitter side, showing similar diversity order to SISO at high SNR.

Given the relevance of these results, this work provides a new accurate approach in the design of practical UOWC systems under realistic underwater scenarios. However, significant challenges remain in hostile UOWC environments, particularly regarding dynamic pointing errors and

Optics EXPRESS

misalignment. The destabilizing effects of oceanic turbulence and tidal currents can lead to substantial misalignment in non-stationary nodes, such as autonomous underwater vehicles (AUVs) and remotely operated vehicles (ROVs), resulting in performance degradation of the proposed MISO schemes. Therefore, further analysis is needed to assess how pointing errors and misalignment, in combination with oceanic turbulence across different scattering conditions, limit the performance of SRC and GTLS systems.

Funding. Spanish Ministerio de Ciencia, Innovación y Universidades (FPU22/02183); Plan Andaluz de Investigacion, Desarrollo e Innovación (P21_00390).

Acknowledgments. The authors would like to acknowledge the support from the Free-Space Optical Communications Algorithms Laboratory at McMaster University.

Disclosures. The authors declare no conflicts of interest.

Data availability. Data underlying the results presented in this paper are not publicly available at this time but may be obtained from the authors upon reasonable request.

References

1. "UNEXMIN, Autonomous Underwater Explorer for Flooded Mine," [Online]. Available: http://www.unexmin.eu/.
2. "The Sonardyne Site: BlueComm Underwater Optical Communications. Sonardyne International Ltd.," http://www.sonardyne.com/.
3. M. Jahanbakht, W. Xiang, L. Hanzo, *et al.*, "Internet of underwater things and big marine data analytics — A comprehensive survey," IEEE Commun. Surv. Tutorials **23**(2), 904–956 (2021).
4. Y. Guo, M. Kong, O. Alkhazragi, *et al.*, "Current trend in optical internet of underwater things," IEEE Photonics J. **14**(5), 1–14 (2022).
5. Z. Zeng, S. Fu, H. Zhang, *et al.*, "A survey of underwater optical wireless communications," IEEE Commun. Surv. Tutorials **19**(1), 204–238 (2017).
6. H. Zhou, M. Zhang, X. Wang, *et al.*, "Design and implementation of more than 50m real-time underwater wireless optical communication system," J. Lightwave Technol. **40**(12), 3654–3668 (2022).
7. B. Majlesein, A. Gholami, and Z. Ghassemlooy, "Investigation of the scattering noise in underwater optical wireless communications," Sci **3**(2), 27 (2021).
8. R. Boluda-Ruiz, P. Salcedo-Serrano, B. Castillo-Vázquez, *et al.*, "Impact of scattering on secrecy outage probability of underwater optical wireless links," IEEE J. Oceanic Eng. **48**(4), 1362–1372 (2023).
9. P. Salcedo-Serrano, R. Boluda-Ruiz, J. M. Garrido-Balsells, *et al.*, "On the scattering-induced fading for optical wireless links through seawater: statistical characterization and its applications," Opt. Express **29**(23), 37101–37116 (2021).
10. R. Boluda-Ruiz, A. García-Zambrana, B. Castillo-Vázquez, *et al.*, "Impact of angular pointing error on BER performance of underwater optical wireless links," Opt. Express **28**(23), 34606–34622 (2020).
11. R. Boluda-Ruiz, P. Rico-Pinazo, B. Castillo-Vazquez, *et al.*, "Impulse response modeling of underwater optical scattering channels for wireless communication," IEEE Photonics J. **12**(4), 1–14 (2020).
12. M. V. Jamali, A. Mirani, A. Parsay, *et al.*, "Statistical studies of fading in underwater wireless optical channels in the presence of air bubble, temperature, and salinity random variations," IEEE Trans. Commun. **66**(10), 4706–4723 (2018).
13. E. Zedini, H. M. Oubei, A. Kammoun, *et al.*, "Unified statistical channel model for turbulence-induced fading in underwater wireless optical communication systems," IEEE Trans. Commun. **67**(4), 2893–2907 (2019).
14. Z. Vali, A. Gholami, Z. Ghassemlooy, *et al.*, "Modeling turbulence in underwater wireless optical communications based on monte carlo simulation," J. Opt. Soc. Am. A **34**(7), 1187–1193 (2017).
15. R. Boluda-Ruiz, P. Salcedo-Serrano, B. Castillo-Vázquez, *et al.*, "Capacity of underwater optical wireless communication systems over salinity-induced oceanic turbulence channels with ISI," Opt. Express **29**(15), 23142–23158 (2021).
16. A. A. Farid and S. Hranilovic, "Diversity gain and outage probability for MIMO free-space optical links with misalignment," IEEE Trans. Commun. **60**(2), 479–487 (2012).
17. R. Boluda-Ruiz, A. García-Zambrana, B. Castillo-Vázquez, *et al.*, "Impact of nonzero boresight pointing error on ergodic capacity of MIMO FSO communication systems," Opt. Express **24**(4), 3513–3534 (2016).
18. E. Lee and V. Chan, "Part 1: optical communication over the clear turbulent atmospheric channel using diversity," IEEE J. Select. Areas Commun. **22**(9), 1896–1906 (2004).
19. R. Priyadarshani, M. R. Bhatnagar, Z. Ghassemlooy, *et al.*, "Effect of correlation on BER performance of the FSO-MISO system with repetition coding over gamma-gamma turbulence," IEEE Photonics J. **9**(5), 1–15 (2017).
20. J. Cheng, C. Tellambura, and N. C. Beaulieu, "Performance of digital linear modulations on weibull slow-fading channels," IEEE Trans. Comm. **52**(8), 1265–1268 (2004).
21. M. V. Jamali, J. A. Salehi, and F. Akhoundi, "Performance studies of underwater wireless optical communication systems with spatial diversity: MIMO scheme," IEEE Trans. Commun. **65**(3), 1176–1192 (2017).

Optics EXPRESS

22. M. V. Jamali, P. Nabavi, and J. A. Salehi, "MIMO underwater visible light communications: Comprehensive channel study, performance analysis, and multiple-symbol detection," IEEE Trans. Veh. Technol. **67**(9), 8223–8237 (2018).
23. H. Jiang, H. Qiu, N. He, *et al.*, "Ergodic capacity and error performance of spatial diversity UWOC systems over generalized gamma turbulence channels," Opt. Commun. **505**, 127476 (2022).
24. X. Chen, Y. Dai, Z. Tong, *et al.*, "Demonstration of a 2x2 MIMO-UWOC system with large spot against air bubbles," Appl. Opt. **61**(1), 41–48 (2022).
25. A. Huang, L. Tao, and Y. Niu, "Underwater wireless optical MIMO system with spatial modulation and adaptive power allocation," Opt. Commun. **412**, 21–27 (2018).
26. M. Elamassie, M. Al-Nahhal, R. C. Kizilirmak, *et al.*, "Transmit laser selection for underwater visible light communication systems," in *30th Annu. Int. Symp. on Pers., Indoor and Mobile Radio Commun.* (IEEE, 2019), pp. 1–6.
27. Q. Zhang, D. Yue, and X. Xu, "Generalized transmit laser selection for vertical underwater wireless optical communications over gamma-gamma turbulence channels," Opt. Express **31**(23), 37943–37958 (2023).
28. B. Zhou, P. Wang, W. Pang, *et al.*, "Effective secrecy throughput optimization for GTLS-based UWOC systems with eavesdropper outage constraint," Opt. Express **32**(18), 32079–32093 (2024).
29. I.-Y. Choi, W.-H. Shin, and S.-K. Han, "CSI estimation with pilot tone for scintillation effects mitigation on satellite optical communication," Opt. Commun. **435**, 88–92 (2019).
30. H. Du, Y. Deng, J. Xue, *et al.*, "Robust online CSI estimation in a complex environment," IEEE Trans. Wireless Commun. **21**(10), 8322–8336 (2022).
31. A. Elfikky and Z. Rezki, "Symbol detection and channel estimation for space optical communications using neural network and autoencoder," Trans. Mach. Learn. Comm. Netw. **2**, 110–128 (2024).
32. A. Garcia-Zambrana, C. Castillo-Vazquez, B. Castillo-Vazquez, *et al.*, "Selection transmit diversity for FSO links over strong atmospheric turbulence channels," IEEE Photonics Technol. Lett. **21**(14), 1017–1019 (2009).
33. A. García-Zambrana, B. Castillo-Vázquez, and C. Castillo-Vázquez, "Asymptotic error-rate analysis of fso links using transmit laser selection over gamma-gamma atmospheric turbulence channels with pointing errors," Opt. Express **20**(3), 2096–2109 (2012).
34. A. Bhowal and R. S. Kshetrimayum, "Transmit laser selection for two hop decode and forward FSO communication with pointing errors," IEEE Commun. Lett. **23**(12), 2301–2305 (2019).
35. M. Elamassie and M. Uysal, "Asymptotic performance of generalized transmit laser selection over lognormal turbulence channels," IEEE Commun. Lett. **24**(8), 1762–1766 (2020).
36. C. Gabriel, M.-A. Khalighi, S. Bourennane, *et al.*, "Monte-Carlo-based channel characterization for underwater optical communication systems," J. Opt. Commun. Netw. **5**(1), 1–12 (2013).
37. Y. Ata and O. Korotkova, "Absorption, scattering, and optical turbulence in natural waters," Appl. Opt. **61**(15), 4404–4411 (2022).
38. Y.-H. Pan and S. Aïssa, "Performance analysis of selective space-time coding and selection diversity under perfect and imperfect csi," in *16th International Symposium on Personal, Indoor and Mobile Radio Communications*, vol. 4 (IEEE, 2005), 2371–2375.
39. H. M. Oubei, E. Zedini, R. T. ElAfandy, *et al.*, "Efficient Weibull channel model for salinity induced turbulent underwater wireless optical communications," in *Opto-Electronics and Commun. Conf. and Photon. Global Conf.* (IEEE, 2017), pp. 1–2.
40. Y.-W. P. Hong, W.-J. Huang, and C.-C. J. Kuo, *Cooperative Communications and Networking: Technologies and System Design* (Springer Sci. & Bus. Media, 2010).
41. International Electrotechnical Commission, "Safety of laser products - Part 1: Equipment classification, requirements IEC 60825-1:2014," 2014.
42. M. Dehghani Soltani, E. Sarbazi, N. Bamiedakis, *et al.*, "Safety analysis for laser-based optical wireless communications: A tutorial," Proc. IEEE **110**(8), 1045–1072 (2022).
43. "The fSONA Networks, Inc.," [Online]. Available: http://www.fsona.com
44. A. A. Farid and S. Hranilovic, "Outage capacity optimization for free-space optical links with pointing errors," J. Lightwave Technol. **25**(7), 1702–1710 (2007).
45. V. V. Nikishov and V. I. Nikishov, "Spectrum of turbulent fluctuations of the sea-water refraction index," Inter. J. Fluid Mech. Res. **27**(1), 82–98 (2000).
46. O. Korotkova, N. Farwell, and E. Shchepakina, "Light scintillation in oceanic turbulence," Waves in Random and Complex Media **22**(2), 260–266 (2012).
47. L. Lu, X. Ji, and Y. Baykal, "Wave structure function and spatial coherence radius of plane and spherical waves propagating through oceanic turbulence," Opt. Express **22**(22), 27112–27122 (2014).
48. M. Shangguan, Z. Weng, Z. Lin, *et al.*, "Day and night continuous high-resolution shallow-water depth detection with single-photon underwater lidar," Opt. Express **31**(26), 43950–43962 (2023).
49. J. R. Barry, *Wireless Infrared Communications* (Springer Science & Business Media, 1994), vol. 280.
50. L. C. Andrews, R. L. Phillips, and C. Y. Hopen, *Laser Beam Scintillation with Applications* (SPIE, 2001), vol. 99.
51. S. Hranilovic, *Wireless Optical Communication Systems* (Springer Science & Business Media, 2006).
52. F. D. A. García, F. R. A. Parente, G. Fraidenraich, *et al.*, "Light exact expressions for the sum of weibull random variables," IEEE Wireless Commun. Lett. **10**(11), 2445–2449 (2021).
53. M. K. Simon and M.-S. Alouini, *Digital Communications over Fading Channels*, 2nd ed. (Wiley-IEEE, 2005).

Optics EXPRESS

54. S. Roy, T. M. Duman, V. McDonald, *et al.*, "High-rate communication for underwater acoustic channels using multiple transmitters and space-time coding: Receiver structures and experimental results," IEEE J. Oceanic Eng. **32**(3), 663–688 (2007).
55. C. Pelekanakis, M. Stojanovic, and L. Freitag, "High rate acoustic link for underwater video transmission," in *Oceans 2003*, vol. 2 (IEEE, 2003), pp. 1091–1097.
56. H. A. David and H. N. Nagaraja, *Order Statistics*, 3rd ed. (John Wiley and Sons Inc., 2003).
57. J. van Campenhout and T. Cover, "Maximum entropy and conditional probability," IEEE Trans. Inf. Theory **27**(4), 483–489 (1981).
58. J. Shore and R. Johnson, "Axiomatic derivation of the principle of maximum entropy and the principle of minimum cross-entropy," IEEE Trans. Inf. Theory **26**(1), 26–37 (1980).
59. A. Goldsmith, *Wireless Communications* (Cambridge University Press, 2005).
60. Z. Wang and G. B. Giannakis, "A simple and general parameterization quantifying performance in fading channels," IEEE Trans. Commun. **51**(8), 1389–1398 (2003).
61. Wolfram Research, Inc., "The Wolfram functions site," [Online]. Available: http://functions.wolfram.com
62. A. A. Kilbas, *H-transforms: Theory and Applications* (CRC, 2004).
63. M. C. Jeruchim, P. Balaban, K. S. Shanmugan, *et al.*, "Modeling of communication systems," *Simul. of Commun. Syst.*, 303–462 (1992).